Chinese Chemical Letters 34 (2023) 107388

Contents lists available at ScienceDirect

Chinese Chemical Letters

journal homepage: www.elsevier.com/locate/cclet

Enrichment and analysis of circulating tumor cells by integrating multivalent membrane nano-interface and endogenous enzyme-signal amplification

Mengjiao Wang[a,1], Dayong Li[a,1], Chengjie Duan[a], Jin Jiao[a], Youjing Gong[a], Xiaoping Wang[c,*], Zhongyun Wang[d,*], Yang Xiang[a,b,*]

[a] State Key Laboratory of Pharmaceutical Biotechnology, School of Life Sciences, Nanjing University, Nanjing 210023, China
[b] State Key Laboratory of Natural and Biomimetic Drugs, Peking University, Beijing 100191, China
[c] Department of Neurology, Tongren Hospital, Shanghai JiaoTong University School of Medicine, Shanghai 200336, China
[d] Department of Anesthesiology, The First Affiliated Hospital of Nanjing Medical University, Nanjing 210029, China

ARTICLE INFO

Article history:
Received 11 November 2021
Revised 5 March 2022
Accepted 29 March 2022
Available online 4 April 2022

Keywords:
CTCs
Nano-interface
Alkaline phosphatase dimer
Signal amplification
Liposomes

ABSTRACT

For circulating tumor cells (CTCs)-based cancer diagnosis and monitoring, effective enrichment and specific analysis of CTCs present significant challenges. The biomembrane interfaces can enhance the high-affinity interactions between various receptors and ligands in life activities by mediating the rearrangement and positioning of membrane-bound components through its fluidity. Inspired by this, we have constructed a multivalent membrane nano-interface using aptamer-linked liposomes for the efficient capture of CTCs. Furthermore, the subsequent introduction of rolling circle amplification (RCA) reaction has increased the number of aptamers and extended them to the surrounding space to improve the affinity of the membrane nano-interface for CTCs. After CTCs are enriched, alkaline phosphatase overexpressed on the surface of tumor cells is used as endogenous enzyme-mediated signal amplification by catalyzing 4-nitrophenyl phosphate (pNPP) with color change, achieving the analysis of CTCs. Finally, the enrichment and visual analysis of human hepatocellular carcinoma (HepG2) with a detection limit of 10 cells/mL can be obtained by integrating the multivalent membrane nano-interface and endogenous enzyme signal amplification. The detection of the target in the serum proved this method has the potential for further clinical application and provides a potential method for studying the correlation between alkaline phosphatase dimer and cancer progression.

Nowadays, cancer is one of the major diseases threatening human health, and more than 90% of cancer deaths are caused by tumor metastasis [1]. As the "seed" of tumor metastasis, circulating tumor cells (CTCs) can provide information from primary tumors and metastatic tumors [2–4], so their identification and analysis have important clinical significance for cancer diagnosis, treatment guidance, and prognostic evaluation [5–8]. The separation and enrichment of CTCs is a prerequisite for subsequent identification and analysis, while the immediate profiling of the captured CTCs can provide accurate information about the tumor in time.

In recent years, affinity-based separation strategies for CTCs have been widely used, which mainly rely on the specific interaction between the recognition ligands (antibodies, peptides, aptamers, *etc.*) on capture interface and biomarkers on CTCs membrane [9–11]. To enhance the interaction between CTCs and capture interface for achieving high efficient separation of CTCs, increasing the affinity of the nano-interface through multivalent binding and nanostructure design has been widely adopted [10,12,13]. However, the existing nano-interfaces usually require the immobilization of recognition ligands on solid substrate, which results in decreased mobility of the recognition ligand on the interface or aggregation when the target biomarker is targeted, thus limiting the enhancement of affinity. In addition, it may lead to nonselective interactions between cells and nano-interface, and the collision damage of target cells [14]. Therefore, achieving efficient, specific and gentle separation and enrichment of CTCs is an urgent problem to be solved, which can avoid misdiagnosis and promote downstream identification and analysis.

The widely existed bio-membrane interface in nature plays an important role in organisms due to its dynamic flow ability [15,16]. For example, the ligand-receptor interaction between bio-

* Corresponding authors.
E-mail addresses: wangxp@ustc.edu (X. Wang), zywang1970@126.com (Z. Wang), xiangy@nju.edu.cn (Y. Xiang).
[1] These authors contributed equally to this work.

https://doi.org/10.1016/j.cclet.2022.03.111
1001-8417/

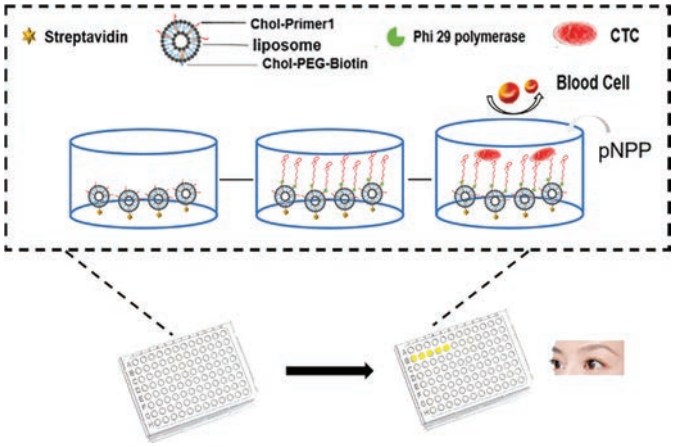

Fig. 1. Schematic illustration of the capture and analysis of CTCs by combining multivalent membrane nano-interface and endogenous enzyme-signal amplification.

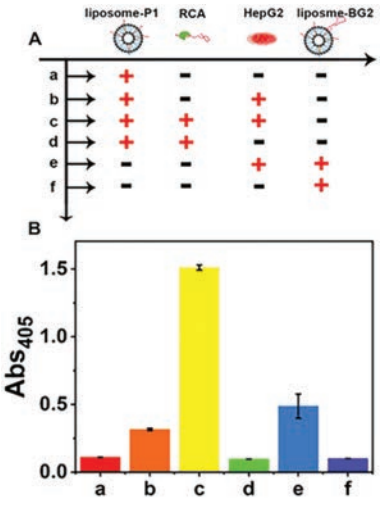

Fig. 2. Feasibility analysis of functionalized membrane nano-interface for enrichment of CTCs. (A) Schematic table of this strategy for cancer cell enrichment under different conditions. (B) The corresponding absorbance at 405 nm in (A).

membrane interfaces can mediate various life activities without destroying each other [17,18]. The lateral fluidity of cell membrane allows the membrane-bound components to rearrange, position, and aggregate in response to the binding of entities with multiple binding sites [19]. The resulted multivalent ligand-receptor interaction greatly enhances the binding affinity in various cell activities, including pathogen attack, cell adhesion, and immune cell-cell recognition [16,20,21]. In the past few decades, various interface engineering strategies have been developed to adjust cell-interface interactions through mimicking natural membrane interfaces, such as controlling interface properties (rigidity, charge, and shape) [22–25] and regulating density, spatial arrangement, and recognition configuration. Some pioneering works have constructed functionalized cell membrane nanovesicle interfaces based on the lateral fluidity characteristics of the membrane interface. Among them, liposomes, as an artificial biological membrane, are widely used because they have the same bilayer structure and fluidity as cell membranes, as well as the advantages of easy-synthesised. With the friendly interaction between the cell and interface, the nanomembrane interface has significant advantages in cell capture and the clinical application of cells-based liquid biopsy [26].

Herein, we have constructed a multivalent membrane nanointerface to capture and analyze CTCs by taking advantages of nucleic acid aptamers as recognition molecules and the biological membrane characteristics of liposomes. Meanwhile, just as octopus has evolved many tentacles as hunting tools by extending their tentacles to the distant space, we have imitated the multivalent tentacles of octopus to maximize the capture efficiency of the membrane nano-interface by RCA-mediated increase of aptamers and spatial extension. Finally, using the catalytic activity of alkaline phosphatase overexpressed on the surface of tumor cells to catalyze the 4-nitrophenyl phosphate (pNPP), the color change of the reaction can be easily observed with the eyes.

As illustrated in Fig. 1, we have reported a soft and multivalent membrane nano-interface for high-performance CTCs isolation. First of all, the Chol-P1 and Chol-PEG-Biotin functionalized nanoparticles have been modified in a 96-well plate through the interaction of biotin-streptavidin. Then, using Chol-P1 as a primer and CT as a template, an RCA reaction has been performed to generate an amplified product rich in placental alkaline phosphatase-intestinal alkaline phosphatase (PLAP-IAP) heterodimer aptamer sequence. The PLAP-IAP heterodimer aptamer sequence is an artificially screened oligonucleotide sequence termed BG2 aptamer that can specifically bind to PLAP-IAP heterodimer. Just like the antennae of an octopus, the amplified product not only increases the number of aptamers, but also extends the aptamers to the surrounding space, which enhanced the affinity with tumor cells overexpressing PLAP-IAP heterodimer and is beneficial to enrichment of CTCs. According to the literature, PLAP-IAP heterodimers may be a potential cancer biomarker because it overexpressed on the surface of many cancer cell lines [27]. At the same time, most protein dimers are assembled through protein-protein interactions, which are usually broken down during cell lysis and protein separation. Although most experimental techniques can separate and detect protein dimers (such as PAGE), there is still a lack of probes that can directly target and recognize in situ. Therefore, PLAP-IAP heterodimer, as a tumor cell surface marker, can single in situ target CTCs overexpressing PLAP-IAP heterodimer, which provides a certain way for further study of its relationship with malignant tumors. Meanwhile, alkaline phosphatase also has catalytic activity and can catalyze the reaction of the substrate pNPP to produce color changes. Using this characteristic of alkaline phosphatase, we can immediately identify and analyze CTCs after achieving CTCs capture and enrichment.

To clearly demonstrate whether our strategy can work for capturing and highly analyzing CTCs, we have employed human hepatocellular carcinoma cell line (HepG2) as a model which highly express PLAP-IAP heterodimer. Then, we have verified that HepG2 as PLAP-IAP heterodimer positive cells can be catalyzed by pNPP (Fig. S1 in Supporting information). Next, in order to confirm whether multiple BG2 aptamer squence to efficiently capture CTCs can be obtained by RCA amplification, a native PAGE assay has been implemented. As shown in Fig. S2 (Supporting information), lane 7 exhibited a distinct single band, indicating the successful execution of the target-cycling RCA in response to the target Primer 1.

As shown in Fig. S3 (Supporting information), in order to obtain a suitable bare blank liposome, we characterize its morphological appearance by transmitting electron microscopy (TEM). It can be seen in the TEM diagram, and the circular state of the liposome of about 150 nm can be seen. At the same time, we also measure the size of the DOPC liposome by NanoSight, as shown in Fig. S4 (Supporting information), we can observe the average diameter of the DOPC liposome is 145.1 nm, which is consistent with the results observed in TEM. In addition, the concentration of the DOPC liposomes we have obtained is about 2.21×10^9 mL^{-1} by NanoSight.

As shown in Fig. 2, in order to verify whether the constructed functionalized membrane nanointerface can be further enriched in CTCs after RCA amplification, we employ the liposomes that are

separately modified with P1, the surface of liposomes-P1 is amplified by RCA, the liposomes only modified with BG2 aptamers and HepG2 cells. Then, the feasibility analysis is verified by the following experiments. We can observe in Fig. 2 that RCA at the functionalized membrane nano-interface can be used for HepG2 enrichment, while the liposomes functionalized P1 alone cannot capture HepG2 cells. At the same time, we also want to know whether the constructed multivalent membrane nano-interface has a better enrichment effect than the single-site membrane nano-interface. The results show that the simultaneous RCA amplification is compared with the nano-interface modified with the BG2 aptamer alone. The capture efficiency of the multivalent nanomembrane interface is about 3.1 times that of single-site membrane nano-interface. The membrane interface has a better enrichment effect. The absorbance results at 405 nm in Fig. 2B have been recorded. First of all, as the experimental group, group c has successfully constructed the multivalent membrane nano-interface and the target cell HepG2. After adding pNPP, it can produce a higher absorbance value at 405 nm. As a control, when HepG2 cells were not added, a lower absorbance value was detected. Similarly, the control group of the nano-interface of the multivalent film was not successfully constructed, and the detected absorbance value was much lower than that of the experimental group. Therefore, all the results have been proved that the multivalent sites constructed by RCA amplification at the membrane nano-interface have an enhanced effect on the enrichment of HepG2.

We have also investigated the effects of several key experimental conditions on the assay performance of our strategy, including RCA amplification time, incubation time of BG2 aptamer and CTCs. In order to minimize the use of reagents and reduce the assay time, we carried out experiments as follows. We then optimize the RCA amplification time on the sensing performance (Fig. S5A in Supporting information), the absorbance responses intensity increases proportionally with the amplification time and starts to reach a plateau at ~60 min and obvious color changes are visualized with increasing RCA amplification time. We reason that, above 60 min, RCA amplification leads too longer aptamers which result in steric hindrance to cause folding and entanglement which affected the combine of BG2 aptamer and CTCs. Therefore, we chose an amplification time of 60 min for RCA events in the subsequent experiments. Next, we studied the effect of the incubation time between BG2 aptamer and CTCs (Fig. S5B in Supporting information), the absorbance at 405 nm first increased with the increase of incubation from 0–20 min but then decreased at incubation time (20–90 min). We conjectured that when the incubation time is longer than 30 min, the binding sites may have combined all CTCs. Given that we want to minimize the assay time, we chose an incubation time of 20 min for sensing performance in the subsequent experiments. The photographs of the catalytic products of APs by pNPP are inserted in Fig. S5 (Supporting information), which further verifies the results.

In order to prove the versatility of this strategy, in addition to HepG2 cells, we also selected human low-metastatic liver cancer cells (MHCC97-L), human breast cancer cells (MDA-MB-231), human cervical cancer cells (HeLa), and normal liver cells (L-02) and set up a mixed group. As shown in Fig. 3, this strategy is universally validated in different cancer cell lines. We find that this strategy can be used for the detection of HepG2, MDA-MB-231 and HeLa cells, while the detection absorbance of MHCC97-L and L-02 cells is low, which shows that this strategy can be used in a wide range of applications in detecting CTCs. It can also proves that our method can enrich and detect the alkaline phosphatase heterodimer protein highly expressed on the surface of CTCs. In addition, the highest absorbance value of HepG2 cells also shows that its target protein expression is higher than that of the other two kinds of cells. As a control, the detected absorbance values of

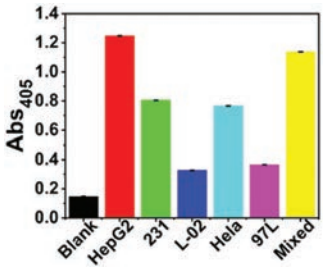

Fig. 3. This strategy is universally validated in different cancer cell lines. The concentration of cell is 1.0×10^5 cells/mL.

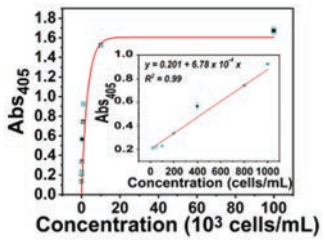

Fig. 4. Quantitative detection of HepG2 cells (0,10,100, 200, 400, 800, 1000, 10^4, and 10^5 cells/mL). Ilustration: Linear relationship of absorbance and HepG2 cells at 405 nm. Error line represents the standard deviation of three independent repetition tests.

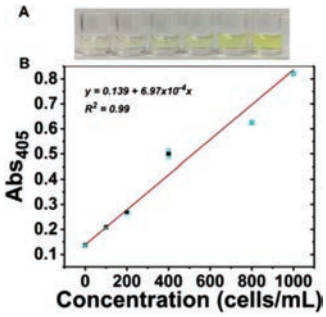

Fig. 5. The oxidation product produced by the captured CTCs catalyzed pNPP was absorbed at 405 nm. (A) Responding to the visual color change of different concentrations of HepG2 cells in 100% serum. (B) The correlation curve of the absorption intensity at 405 nm in 100% serum.

MHCC97-L and L-02 cells are low. The higher detection absorbance value of the mixed group further indicates that this strategy can be used to detect CTCs in a wide range of applications.

Under optimized conditions, we have examined the application of this proposed strategy for CTCs' analysis. To characterize the analysis performance, we operated on different concentrations of live cancer cells, we then tested different concentrations of HepG2 cells in the buffer (Fig. 4). The absorbance values of the catalytic products of APs by pNPP are plotted in Fig. 4 after the addition of HepG2 cells ranging from 0 to 1.0×10^5 cells/mL. It can be visualized that the absorbance value gradually increases with the increasing amount of target cells. Moreover, the absorption intensity and cell concentration have a positive linear correlation with a linear response range from 10 to 1000 cells/mL, and the detection limit is 10 cells/mL. Because of the excellent capture and analysis efficient, this strategy was applied to the complex environment and the potential application in clinical diagnosis. We have designed a standard addition method by adding different concentrations of HepG2 cells into 100% undiluted human serum. As a result, the absorbance at 405 nm is measured to be proportional to HepG2 cells concentration (Fig. 5) and obvious color changes are visualized with increasing the concentration of HepG2 cells,

demonstrating that the proposed strategy is expected to be used to detect CTCs in complex biological samples.

In this work, we have designed and proposed a method that combines multivalent membrane nano-interface and endogenous enzyme signal amplification techniques to effectively capture and specificize CTCs. At the same time, the feasible of this method is verified by HepG2 cells as a model. To simulate cellular interactions between cell membrane interfaces, P1-liposomes are modified to the pore substrate for forming nano-interface. Besides we construct a multivalent membrane by RCA reaction. The results show that this multi-valent biomimetic nanointerface reaches about 3 times as much as a single-nanointerface, and reduces the background signal to some extent because of its the structure and function of a natural biomembrane. Finally, by using endogenous enzyme AP, the catalytic reaction product of pNPP is quantified, so this method can be used as a high-level capture method of CTCs. While ensuring the integrity of the cells and non-destructiveness, it is expected to be used for non-capture cells and further analyze the CTCs.

Declaration of competing interest

The authors report no declarations of interest.

Acknowledgments

This work is supported by the National Natural Science Foundation of China (No. 81672570), and the State Key Laboratory of Natural and Biomimetic Drugs (No. K202009).

Supplementary materials

Supplementary material associated with this article can be found, in the online version, at doi:10.1016/j.cclet.2022.03.111.

References

[1] S. Valastyan, R.A. Weinberg, Cell 147 (2011) 275–292.
[2] G. Siravegna, S. Marsoni, S. Siena, A. Bardelli, Nat. Rev. Clin. Oncol. 14 (2017) 531–548.
[3] M. Ignatiadis, M. Lee, S.S. Jeffrey, Clin. Cancer Res. 21 (2015) 4786–4800.
[4] M. Mohme, S. Riethdorf, K. Pantel, Nat. Rev. Clin. Oncol. 14 (2017) 155–167.
[5] L. Keller, K. Pantel, Nat. Rev. Cancer 19 (2019) 553–567.
[6] M. Yu, A. Bardia, N. Aceto, et al., Science 345 (2015) 216–220.
[7] V. Plaks, C.D. Koopman, Z. Werb, Science 341 (2013) 1186–1188.
[8] K. Pantel, C. Alix-Panabières, Nat. Rev. Clin. Oncol. 16 (2019) 409–424.
[9] T.H. Kim, Y. Wang, C.R. Oliver, et al., Nat. Commun. 10 (2019) 1478.
[10] H.J. Yoon, A. Shanker, Y. Wang, et al., Adv. Mater. 28 (2016) 4891–4897.
[11] E.S. Johnson, S. Xu, H.-M. Yu, et al., Anal. Chem. 91 (2019) 14605–14610.
[12] J. Dong, Y.J. Jan, J. Cheng, et al., Sci. Adv. 5 (2019) eaav9186.
[13] M.H. Park, E. Reátegui, W. Li, et al., J. Am. Chem. Soc. 139 (2017) 2741–2749.
[14] L. Wu, H. Ding, X. Qu, et al., J. Am. Chem. Soc. 142 (2020) 4800–4806.
[15] D. Marguet, P.F. Lenne, H. Rigneault, H.T. He, EMBO J. 25 (2006) 3446–3457.
[16] B.M. Mognetti, P. Cicuta, L. Di Michele, Reports Prog. Phys. 82 (2019) 116601.
[17] S. Ballweg, E. Sezgin, M. Doktorova, et al., Nat. Commun. 11 (2020) 1–13.
[18] Y. Lin, L. Jiang, Y. Huang, et al., Chem. Commun. 55 (2019) 5387–5390.
[19] D. Carradori, A.G. dos Santos, J. Masquelier, et al., J. Control. Release 292 (2018) 248–255.
[20] J.B. Huppa, M. Axmann, M.A. Mörtelmaier, et al., Nature 463 (2010) 963–967.
[21] D.E. Handy, R. Castro, J. Loscalzo, Circulation 123 (2011) 2145–2156.
[22] J. Li, C. Qi, Z. Lian, et al., ACS Appl. Mater. Interfaces 8 (2016) 2511–2516.
[23] W. Wang, H. Cui, P. Zhang, et al., ACS Appl. Mater. Interfaces 9 (2017) 10537–10543.
[24] Y. Hao, Y. Li, F. Zhang, et al., ChemPhysChem 19 (2018) 2046–2051.
[25] C.H. Dr, G. Yang, Q. Ha, J.M. Dr, S.W. Prof, Adv. Mater. 27 (2015) 310–313.
[26] L. Wang, Y. Pan, Y. Liu, et al., ACS Appl. Mater. Interfaces 12 (2020) 322–329.
[27] T. Bing, L. Shen, J. Wang, et al., Adv. Sci. 6 (2019) 1900143.